Construction and Building Materials 281 (2021) 122612

Contents lists available at ScienceDirect

Construction and Building Materials

journal homepage: www.elsevier.com/locate/conbuildmat

High-performance cementitious grout with fly ash for corrosion protection of post-tensioned concrete structures

Manu K. Mohan, Radhakrishna G. Pillai *, Manu Santhanam, Ravindra Gettu

Department of Civil Engineering, Indian Institute of Technology Madras, Chennai, India

HIGHLIGHTS

- High-performance grout for the corrosion protection of post-tensioned (PT) tendons was developed.
- Developed grout is made with two fly ashes to improve the packing density and fluidity.
- Developed grout has excellent resistance against shrinkage and the formation of voids, bleedwater and softgrout.
- A set of stringent performance specifications for PT grouts are developed.

ARTICLE INFO

Article history:
Received 27 October 2020
Received in revised form 23 January 2021
Accepted 3 February 2021
Available online 28 February 2021

Keywords:
Post-tensioned
Concrete
Grout
Tendons
Fluidity
Bleed
Rheology
Shrinkage
Performance specifications

ABSTRACT

In order to provide corrosion protection of tendons in post-tensioned (PT) concrete systems, the congested interstitial spaces between the strands and duct are ideally to be filled with cementitious grouts. However, many currently used grouts do not have the desired fluidity and resistance to segregation – leading to formation of voids, frothy grout materials, and premature corrosion of strands. This paper presents a 3-phase study on the development of high-performance, pre-blended grouts. Several grouts were formulated with various proportions of ordinary portland cement (OPC), fly ash and chemical admixtures. The fluidity, bleed (i.e., standard, wick-induced, pressure-induced, and -inclined tube), softgrout, rheological, and shrinkage parameters of the formulated grouts were assessed; based on which a systematic selection of grouts was performed in three phases. Finally, a grout with 52 and 48% of OPC and fly ash, respectively (by volume) and optimal dosages of chemical admixtures was formulated and pre-blended in an industrial facility. This grout satisfies a set of performance specifications on fluidity, resistance against segregation (say, bleedwater and softgrout formations), and shrinkage. Therefore, the grout is capable of filling the ducts and providing long-term corrosion protection of PT strands.

1. Introduction

Grouted, post-tensioned ('PT' herein) concrete systems with seven-wire strands are commonly used in the construction of long-span segmental bridges, high rise buildings, nuclear vaults, water retaining structures, etc. Some of these structures are designed for a corrosion-free service life of about 100 + years and are exposed to the chloride-rich environment and other aggressive conditions (say, moisture, marine, de-icing/anti-icing salts, carbonation, etc.). Such aggressive conditions can cause corrosion of the pre-stressing strands, if they are not protected adequately [1]. In general, multiple levels of protection systems are used to protect the strands from corrosion [2]. Among these, the cementitious grouts for post-tensioning application ('PT grouts' herein) are considered as the most important level of protection [3]. Therefore, to achieve long corrosion-free service life, the quality of PT grouts and complete filling/grouting of ducts are of utmost importance.

1.1. Strand corrosion due to voids, bleedwater, softgrout formation

Premature corrosion and failure of strands/tendons have been documented in many PT concrete structures around the world (see Table 1) [4–12]. Many of these structures experienced severe corrosion of strands within short periods (say, within 5 to 30 years after the construction, which is much earlier than the expected corrosion-free service life). The major reported reason for the strand corrosion was the presence of unwanted voids inside the ducts, especially at/near the anchorages [13,14]. These voids are mainly formed due to the poor grouting practices and the use of grouts with low bleed resistance - resulting in the accumulation of bleed-water at high points of the tendons (say, anchorages

* Corresponding author.
E-mail address: pillai@iitm.ac.in (R.G. Pillai).

https://doi.org/10.1016/j.conbuildmat.2021.122612
0950-0618/

Nomenclature

$\tau, \dot{\gamma}, \tau_0$:	Shear stress, shear rate, and yield stress, respectively
$AS_{t,\ days}$:	Autogenous shrinkage strain at 't' days
$BV_{inclined}$:	Bleed volume in inclined tube test
$BV_{pressure,\ P}$:	Bleed volume in pressure-induced bleed test (at pressure 'P')
$BV_{standard}$:	Bleed volume in standard bleed test
BV_{wick}:	Bleed volume in wick-induced bleed test
bvob:	by volume of binder
bvog:	by volume of grout
bwob:	by weight of binder
$D_{s,\ T}$:	Spread diameter, 'T' minutes after mixing
FaF1:	Class F fly ash 1
FaF2:	Class F fly ash 2
$f_{c,\ t}$:	Cube compressive strength at 't' days of curing (here t = 3, 7, 28)
HRWR:	High range water reducer
OPC:	Ordinary Portland cement
PBG:	Pre-blended grout
PCG:	Plain cement grout
PPG:	Pre-packaged grout
PT:	Post-tensioned
SBG:	Site-Batched-Grout
SRA:	Shrinkage reducing admixture
ST_{final}:	Final setting time
$ST_{initial}$:	Initial setting time
$T_{e,\ T}$:	Efflux time at 'T' minutes after mixing
VMA:	Viscosity modifying agent
$V_{softgrout}$:	Volume of softgrout

Table 1
Tendon failure/corrosion incidents in PT structures.

Name of the PT structure [Reference]	T_{corr} in years* [year]
Bickton Meadows bridge, UK [2]	15 (1967)
Angel Road bridge, UK [2]	30 (1980)
Berlin Congress hall, Germany [4]	23 (1980)
Taf Fawr bridge, UK [2]	21 (1982)
Ynsys-y-Gwas bridge, UK [5]	33 (1985)
Mandovi River bridge, India [6]	12 (1986)
Folly New bridge, UK [2]	30 (1988)
Melle bridge, Belgium [7]	13 (1992)
Bob Graham bridge, USA [8]	08 (1995)
Niles Channel bridge, USA [9]	16 (1999)
Lowe Speedway bridge, USA [10]	05 (2000)
Mid-Bay bridge, USA [11]	09 (2001)
Varina-Enon bridge, USA [12]	17 (2007)
Ringling Causeway bridge, USA [13]	08 (2011)

* T_{corr} - time taken (in years) for tendon corrosion to occur and the values in parenthesis indicate the year at which the corrosion was observed or failure occurred.

and crests of the tendons). Later, this bleed-water gets reabsorbed by the hardened grout or evaporated – creating unwanted voids at/near the anchorage zones and other high points and leading to exposed the strands. Also, such voids facilitate the easy access to moisture, oxygen, chloride, carbon dioxide, etc. to the tendons – leading to the onset of strand corrosion [15].

In the last two decades, the grout industry has developed shrinkage-compensating and non-shrink cementitious grouts with low bleedwater formation. However, such grouts often exhibit the formation of softgrout (frothy and porous material), which segregate/float/settle at the top portion of the ducts, especially near the anchorage zones (see Fig. 1). This softgrout facilitates the collection of moisture, chloride etc. and accelerate corrosion of strands, especially at the anchorage zones. Once initiated, corrosion can propagate due to the formation of electrochemical cells between the small anodic regions (say, the exposed and corroding strand portions) and the larger cathodic regions (say, strand portions covered with cementitious grout) [15]. The smaller anode-to-cathode ratio (i.e., with the presence of small voids) leads to a higher localized corrosion rate – resulting in localized reduction of the cross-section of the strand. Hence, to achieve the desired corrosion protection of strands, even the smallest interstitial spaces between the strands and duct must be filled with cementitious grout. Literature also suggest that the corrosion of strands in inclined or vertical PT systems can be severe. It is also reported that strand corrosion could significant impact the serviceability and flexural reliability of PT bridge girders [16,17].

Fig. 2 shows the schematic representation of a typical segmental PT concrete bridge with internal grouted tendons. At Section A-A (i.e., at/near the support) of the bridge girder, the strands get pulled towards the top of the duct (say, eccentric and congested strands) leading to difficulty in covering the strands with grout. This scenario also provides a clear path (at the bottom of the duct) for an easy free flow of grout. Similarly, at Section B-B at mid-span of the bridge girder, the strands get congested at the top portion inside the duct. In this case, it is very difficult to completely fill the interstitial spaces between the strands and the duct, unless the grout is highly fluid and resistant against bleed-water and softgrout formation.

1.2. Fluidity and its retention of grouts

The grout must be fluid enough in the beginning and must retain its fluidity until the grouting operations are completed – i.e., until the smallest interstitial spaces and narrow paths between the strands and between the strands and duct are filled, which might take about 3 h in a typical grouting operation. Also, higher the fluidity, lower will be the required pumping pressure. The fluidity of the PT grouts is usually assessed by measuring the 'efflux time' using the Marsh cone with different orifice diameters [19,19]. As the interstitial space and paths in PT systems could be much smaller and corresponds to different flow conditions, Marsh cone tests with a smaller orifice diameters were also reported in literature [21–23]. Fluidity can also be assessed by measuring the 'spread diameter' of freshly prepared grout, as per EN 445 [18]. The spread test can also help in visually assessing the segregation, if any, along the periphery of the spread grout.

Literature indicates that the replacement of OPC with fly ash up to 40% can enhance the fluidity and its retention – mainly due to the ball-bearing effect of the spherical fly ash particles and reduced rate of hydration [25,25]. In addition to that the use of fly ash could be beneficial for protecting the strands against corrosion as it was reported that the chloride binding capacity of cementitious systems increases with the increase in fly ash replacement level up to 50%. This could be due to the higher alumina content in fly ash, which results in the formation of Friedel's salt in these systems [27,27]. Site-batched grouts (SBGs) with superplasticizer and high water content (say, w/b greater than 0.40) are commonly used, which exhibit excellent fluidity but also significant bleeding [28]. However, such grouts could pass the Marsh cone test, which is

a) Opened anchorage end (adapted from [18])

b) A layer of highly permeable softgrout with a ruler pierced into it (adapted from [13])

Fig. 1. Different types of grouts observed in PT bridges in the USA.

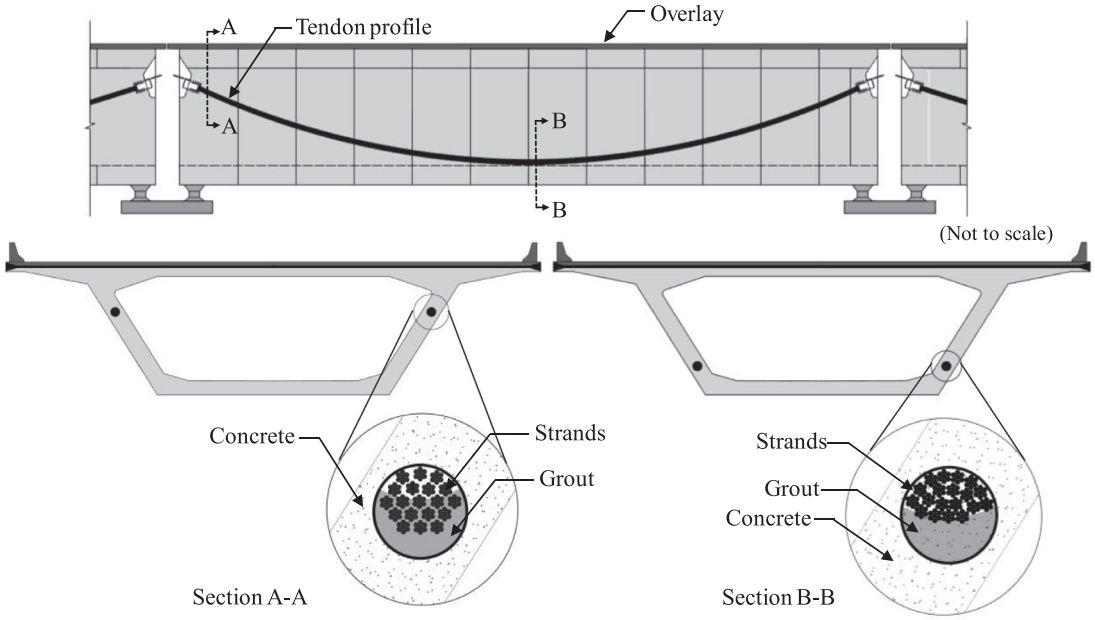

Fig. 2. A typical tendon profile in a simply supported post-tensioned bridge – showing the possible void locations and conditions.

sometimes the only test used for qualifying grouts at most construction sites. Obviously, such inappropriate approach of using only Marsh cone tests can result in the selection of plain cement grouts (PCGs) and SBGs, which are non-thixotropic and exhibit low resistance to bleed/segregation – a case of "false-positive" result. Therefore, the Marsh cone test alone should not be used as a screening test for the PT grouts and the bleed resistance must be considered while assessing PT grouts [28]. Also, grouts exhibiting longer efflux time may be accepted as long as they are able to fill the interstitial spaces between the strands and duct, and the bleed resistance and other properties are met.

1.3. Segregation resistance of grouts

Two major issues associated with segregation of PT grouts is the formation of bleed-water and softgrout, the latter being a recently observed problem associated with some of the pre-packaged grouts containing inert fillers [30,30]. The issues associated with bleedwater formation has been reported since the early 1970 s [31]. Bleed resistance of PT grouts can be measured by the standard bleed test and wick-induced bleed test [18], (see Fig. 3a and 3b), that can be performed at grouting sites. The standard bleed test gives the amount of bleed-water (in a cylinder with fresh grout) at 3 h of stagnation. In a bridge tendon, the presence of long capillary paths between the seven wires in a strand and between the congested, stressed strands can lead to significant amount of bleed-water in tendons could be significant - due to the presence of strands. Hence, the wick-induced bleed test with a single strand inside a cylinder of fresh grout gives a better estimate of bleed water than the standard bleed test. Further, in the tendons with congested multi-strands, the amount of wicking and bleed-water could be significant. The inclined-tube bleed test (see Fig. 3c) [18] with a similar proportion of cross-section of strands inside a duct can provide a closer estimate of bleeding in bridge tendons. If the PT system has significant inclined profile (say, at the end regions of deep girders) or vertical profile (say, in tall columns),

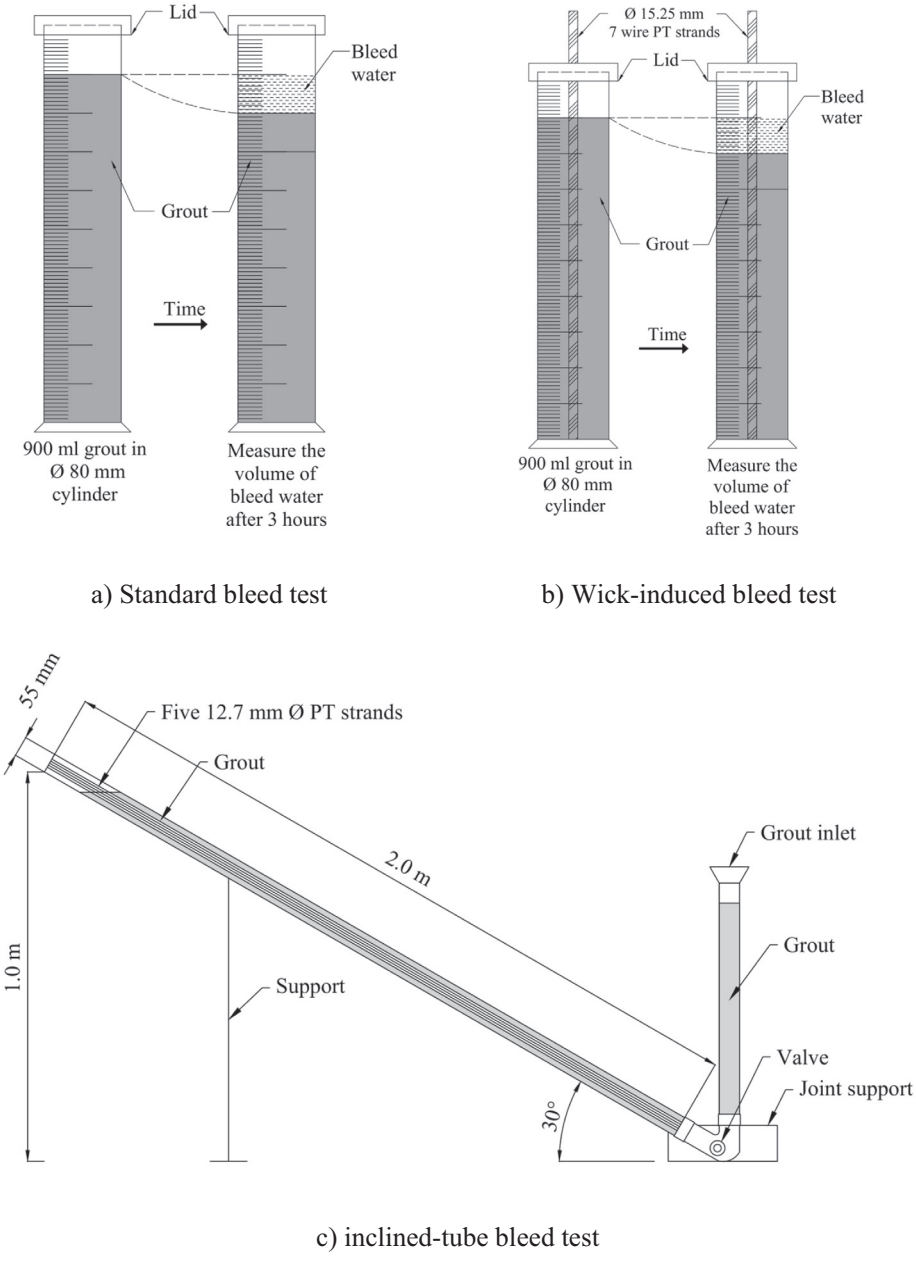

Fig. 3. Schematic illustration of the test methods to measure the bleed water volume.

then the pressure-induced bleed test [32] should also be conducted to get a better estimation of bleed water that could form in such cases [32,33].

The use of supplementary cementitious materials (SCMs) and multiple chemical admixtures to reduce bleeding of grouts has also been widely studied [26,34]. The viscosity modifying agents (VMAs) can increase the viscosity of the liquid phase of the grout, which in turn can enhance the bleed resistance; however, reduces fluidity [34]. Different classes of VMAs, such as cellulose ethers and natural gums, have been used in PT grouts for achieving the desired bleed resistance [35,35]. Also, studies show that the use of nanoclay could improve the stability as well as the robustness of the cementitious mixtures [37,37]

Softgrout forms due to the differential settlement of various particles (including the inert fillers) because of the difference in density and delayed setting [31,38]. The addition of inert filler materials (say, limestone powder) of up to 35–45% of the total binder resulted in significant amount of softgrout [30]. Softgrout allows easy access to the deleterious materials leading to premature corrosion of strands [13]. Therefore, utmost care should be taken while selecting the filler material and the level of replacement. In short, a high performance PT grout with good resistance to segregation (i.e., bleeding and softgrout formation) is necessary for achieving long term corrosion protection.

1.4. Shrinkage resistance of grouts

PT grouts must also be sufficiently resistant against shrinkage and cracking. This could be achieved by using (i) shrinkage compensating grouts or (ii) non-shrink grouts. The shrinkage-compensating grouts work by slowly imparting an expansion at an early age, which can compensate the instantaneous shrinkage.

In the past, aluminium powder, which reacts with hydroxide ions in grouts and releases hydrogen gas leading to expansion has been used [31]. However, nowadays, the use of aluminum powder is prohibited due to the possibility of hydrogen embrittlement of pre-stressed strands [39]. On the other hand, non-shrink grouts utilize shrinkage reducing agents (SRAs) that can reduce the surface tension of the liquid phase in the fresh grout. SRA particles are surfactants that are essentially amphiphilic and align in such a way that the hydrophilic part is in water and hydrophobic part in the air. Consequently, the interfacial energy between air and water can reduce as the intermolecular forces between the SRA and water reduce [40]. Also, the concentration of SRA at which micelles (or flocs) of SRA particles starts forming is called the critical micelle concentration (CMC). Beyond CMC, excessive micelle formation happens, and surface tension may not reduce further [40]. The lesser the surface tension of the liquid phase in the capillary pores, the less will be the shrinkage, in general [42–43]. SRAs are very efficient in reducing the autogenous shrinkage in pure and blended cement pastes [45–47]. For example, the use of 2% bwob glycol-based SRA by weight of binders can reduce the autogenous shrinkage of PT grouts by about 56% [48].

2. Research significance

Corrosion protection of post-tensioned concrete systems requires the use of high performance grout for completely filling the duct/tendon systems. Site-batched grouts used at many sites exhibit good fluidity but not sufficient resistance to bleedwater formation, which can result in the formation of voids in the ducts and premature corrosion of strands. Most pre-packaged grouts in the market exhibit excellent bleed resistance but low resistance to softgrout formation, which can lead to premature corrosion of strands. This research was aimed at developing a pre-blended cementitious grout using ordinary portland cement, fly ash and chemical admixtures to meet the desired requirements of fluidity and its retention, resistance to the formation of bleedwater and softgrout, and resistance to shrinkage. Therefore, this grout is expected to provide long-term corrosion protection in PT concrete systems, which will lead to a lower life cycle cost.

3. Experimental program

3.1. Overview of the experimental program

The experiments were conducted in three phases, as follows (see Fig. 4 for details).

- Phase I: Identification and characterization of suitable raw materials, designing, and characterization of pre-blended grouts (PBGs 1 & 2).
- Phase II: Improving the mixture proportion and characterization of PBG3.
- Phase III: Fine-tuning of the reference grout (PBG3), and industrial-scale blending of the PBGs (i.e., PBGs 4, 5 & 6) and performance assessment.

In Phase I and II, binders and chemical admixtures in powder form were pre-blended using a laboratory scale planetary mixer (Hobart mixer) of 18-litre capacity for 15 min. All the experiments were conducted in a controlled environment (i.e., ambient temperature of 25 °C and relative humidity of 65%) after conditioning the materials for 24 h at the same temperature. The large-scale blending in Phase III was carried out in an industrial blending facility of 3 metric ton capacity.

3.2. Materials

53 Grade OPC conforming to the IS 12,269 [49] and two Class F fly ashes (denoted as FaF1 and FaF2) with different particle size distributions and mean diameters were used. Table 2 shows the chemical composition and physical properties of OPC, FaF1, and FaF2. The particle size distributions of these binders were determined using laser diffraction and is shown in Fig. 5. A polycarboxylic ether (PCE) based high range water reducer (HRWR) and hydroxyethyl methylcellulose (VMA) were used to increase the fluidity and the bleed resistance. A glycol-based shrinkage reducing agent (SRA) was used to reduce the shrinkage of the grout. No inert filler (say, limestone powder, quartz powder, etc.) was used in the mixture to avoid the formation of softgrout.

3.3. Mixing

A custom-made high shear mixer with a drum capacity of 20 L was used. The mixer can rotate at a maximum mixing speed of 3000 rpm with a least count of 5 rpm. For each trial, 25 kg powder grout material was mixed with water and yielded 15–17 L of the grout. The quantity of grout material, mixing speed, and mixing sequence was kept uniform throughout the experiment. Also, the consistency of the grout mixed with the custom-made high shear mixer was controlled by uniform mixture proportioning and mixing procedures across various batches; and it was found that the grout mix exhibited adequate consistency across batches. The following mixing procedure was developed based on the recommendations from standards and literature [29,50,51]. Initially, the mixing water was poured into the mixing bowl. Then, the pre-blended, conditioned grout powder was transferred to the mixing bowl while the blades were rotating at a speed of 300 rpm. The pre-blended grout material was transferred to the mixer gradually to avoid the formation of the lumps and settling of the ingredients. After all the materials were transferred, the mixing speed was increased to 1500 rpm and kept constant for 360 s. The high-speed mixing enabled proper dispersion of the binders and chemical admixtures. After the mixing operation, the grout was tested at 1 min after mixing and at regular intervals of 15 min up to 3 h.

3.4. Methodology

The Puntke test has been used for determining the packing density of binders. The principle of the Puntke test is that the water added to the dry binders will fill all the voids and act as a lubricant to make the material compact efficiently. After all the voids get filled and beyond a particular water content, the excess water will appear on the surface (a glossy appearance of a thin layer of water will be visible on the surface of the mix). One of the advantages of this test is that it can closely simulate the condition of binders in the cement paste/grout, as the test is performed in the wet condition. The packing density ϕ was determined as follows:

$$\phi = 1 - \frac{V_W}{V_W + V_P} \quad (1)$$

where V_P is the volume of powder and V_W is the volume of water.

The fluidity of the grouts was measured by the Marsh cone and spread tests immediately after mixing and up to 3 h, as per EN 445 [18]. The bleed resistance of the grouts was measured using the standard, wick-induced, and inclined-tube bleed tests [18]. The pressure-induced bleed test was carried out by filling a Gelman pressure cell with grout as per ASTM C1741 [32]. The pressure was increased gradually in steps of 70 kPa up to 350 kPa that corresponds to the pressure at the bottom of a 6 m tall grout column. Each pressure increment was sustained for 3 min. The cumulative volume of bleed-water was measured and expressed in percentage

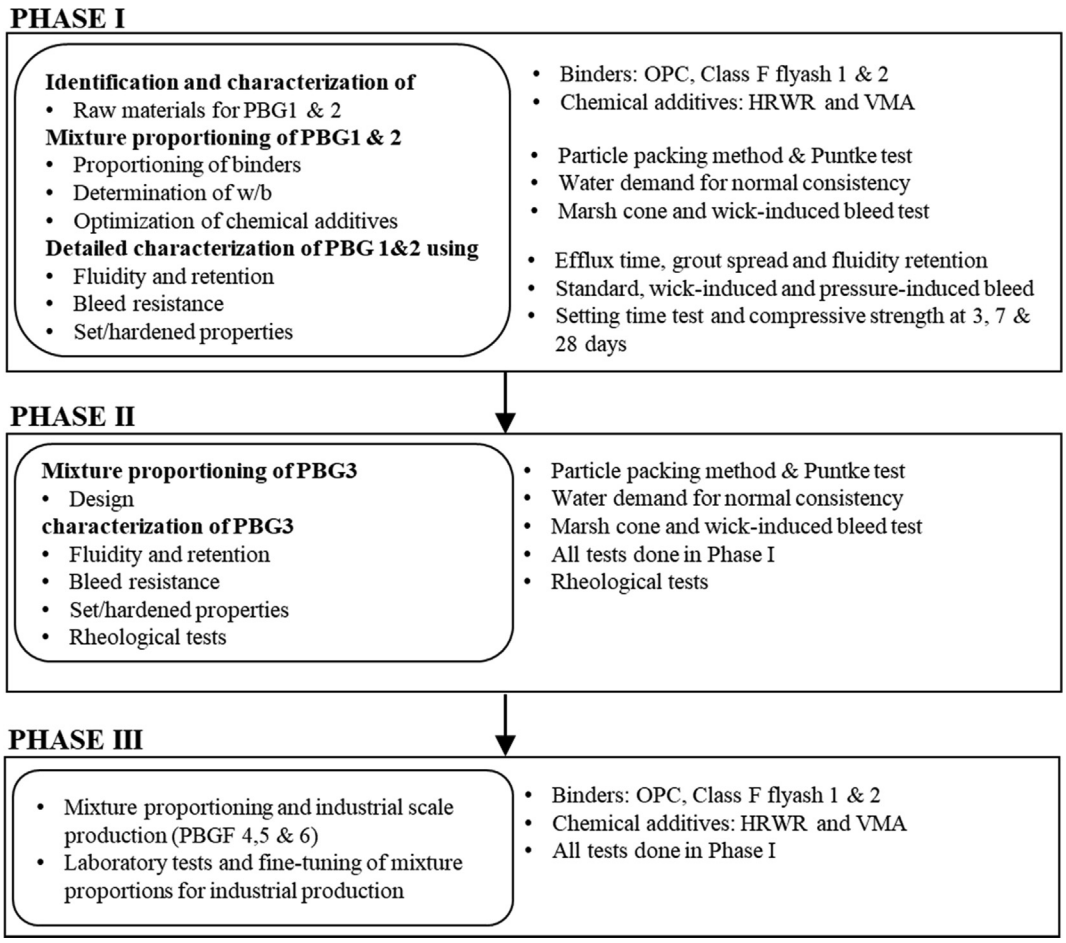

Fig. 4. Different phases of the experimental programme.

Table 2
Chemical composition and physical properties of the binders.

		OPC	FaF1	FaF2
Composition (%)	SiO_2	20.88	59.32	60.56
	Al_2O_3	5.54	29.95	32.67
	Fe_2O_3	4.71	4.32	4.44
	CaO	61.70	1.28	1.41
	MgO	1.06	0.61	0.23
	$(Na_2O)_e$	0.20	0.16	0.12
	LOI	2.27	–	–
Physical properties	Mean diameter (μm)	15	3.0	4.5
	Specific surface area (m^2/kg)	330	536	621
	Specific gravity	3.15	2.34	2.35

by volume of grout (% bvog). The inclined tube test was modified by reducing the total length of the inclined tube from 5 m to 2 m. For all the bleed tests, the open ends of the graduated cylinders and inclined tubes were covered with a plastic lid to avoid evaporation.

The surface tension of the liquid phase of fresh grout was measured using a tensiometer, as per ASTM D1331 [52]. Using a Gelman Pressure cell, about 20 ml liquid was extracted from fresh grouts with different dosages of SRA, and then the surface tension was measured. Also, the shrinkage studies were carried out with hardened grout on 25 × 25 × 285 mm prism specimens, as per ASTM C157 [53]. Immediately after casting, the specimens were covered with a polyethylene sheet to prevent moisture loss. The specimens were demoulded after 24 h and the length was measured. Then, the specimens were stored at 25 °C and 65% relative humidity for 70 days. For determining the autogenous shrinkage, the specimens were wrapped with two layers of aluminium foil. The autogenous and total shrinkage deformations were measured (using an extensometer with a least count of 0.001 mm) for 70 days and change in length were calculated.

The setting time of the PBGs was measured by the time corresponding to a depth of penetration of 35 mm using a Vicat apparatus as per ASTM C953 [54]. The compressive strength of cube specimens after 3, 7, and 28-day curing was determined as per ASTM C942 [55].

The rheological characterization has been carried with Brookfield HA DV II + Pro viscometer attached with a co-axial cylinder geometry (inner cylinder radius = 16.8 mm, gap = 1 mm). The spindle of the co-axial cylinder geometry had about 0.5 mm deep corrugations, which helped in reducing wall slip during the shearing

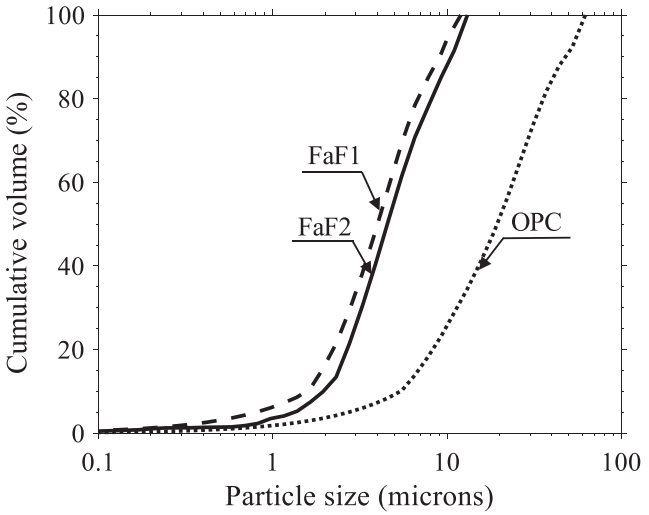

Fig. 5. Particle size distribution curve of all the binders.

stage. The shear strain rate was varied from a low shear strain rate to a relatively high shear strain rate. The gravitational settling was avoided by choosing the period of testing as low as possible. After a pre-shear of 24 s^{-1} for 1 min, shear strain rate was swept from 24 to 90 s^{-1} and then 90 to 24 s^{-1} in steps of 0.5 s^{-1}. The chosen range of shear strain rate could correspond to the shear strain rate during the mixing, pumping, and flow through the duct [56]. Following the procedures in literature [24,57,58], the flow curves were fitted to the Herschel-Bulkley model and parameterized by the yield stress (τ_0), shear rate ($\dot{\gamma}$), apparent viscosity η and an exponent (n), given by:

$$\begin{aligned} \dot{\gamma} &= 0, && \text{if} \quad \tau < \tau_0 \\ \tau &= \tau_0 + \eta\dot{\gamma}^n, && \text{if} \quad \tau \geqslant \tau_0 \end{aligned} \tag{2}$$

4. Results and discussion

This section contains the results of Phases I to III. As discussed in the methodology section, PBG 1 and PBG 2 were designed and characterized using laboratory tests in Phase I. In Phase II, PBG 3 has been designed and the properties were assessed. Then, in Phase III, three grouts were designed (PBGs 4, 5 & 6) and blended on an industrial blender and the properties were assessed. Table 3 provides the composition, fresh properties and hardened properties of all the PBGs formulated in Phases I, II, and III. Mixture proportion of the grouts and their properties are presented in same table to have a comprehensive view for the reader. Also, this will allow the reader to compare the grout compositions with their properties.

4.1. Phase I – PBG 1 & 2

4.1.1. Mixture proportioning (PBG1 & 2)

Good fluidity and resistance against segregation (i.e., bleeding and softgrout formation) and shrinkage can be achieved by maximising the packing density of powder ingredients and the use of appropriate types and dosage of chemical admixtures. It is reported that the total particle packing density can have a linear correlation with the plastic viscosity of the cement paste containing fly ash [59]. Also, as the packing density of grout increases, the yield stress can reduce [60], which means a reduction in the required pumping pressure/energy. The volume proportions of the binders (OPC, FaF1, & FaF2) were optimized through particle packing. EMMA, a commercially-available particle packing software [61] was used for this purpose. Based on the particle size distributions, specific gravity, the proportion of the binders, distribution coefficient, and sizes of the minimum and maximum particles in the system, the software calculates the idealized distribution curve based on the modified Andreasson model [62] and compares with the actual particle size distribution curve. As the grout mix requires very good fluidity, the distribution coefficient should be as low as possible. Based on experience, a distribution coefficient of 0.23 was chosen for obtaining the ideal gradation curves. Different volume proportions of the binders exhibiting maximum packing density were obtained from the software. Then, the volume proportion at which the highest possible packing density is determined.

Considering the short time required to perform the Puntke test, water can be used for assessing the packing density of cementitious powders (i.e., effects due to hydration are neglected) and the binder proportions can be optimized for the desired levels of fluidity. Based on the Puntke tests, the proportion of binders exhibiting the highest packing density was selected. Fig. 6(a) shows the Puntke test results of the mix with OPC and FaF1 (the finer fly ash used). The maximum packing density occurred at a volume replacement of 42% FaF1. Similarly, Fig. 6(b) shows the packing densities of the combinations of OPC and FaF2. The maximum packing density occurred at a volume replacement of 38% FaF2. In both the cases, the addition of HRWR did not change the binder proportion for the maximum packing density. The absolute value of packing density increased when 0.1% bwob HRWR was used, which can be attributed to the increased dispersion of binders, resulting in better compaction [60]. The combinations and proportions of binders exhibiting high packing density, good flow and bleed resistance were chosen for further study.

It is important to keep the water-binder ratio (w/b) as low as possible to reduce the bleeding/segregation. The water demand for normal consistency was determined for all the different binder combinations using the Vicat apparatus [54]. However, at this w/b, the grout may not have the target fluidity needed for the pumping and subsequent flow through the duct. To achieve the desired fluidity, a suitable HRWR can be used as it could increase the fluidity of the grout mixture [64,64]. Though the HRWR generally increases the fluidity of the cement grout, the mechanism of action is different for different types of HRWRs. When the PCE based HRWR used in cementitious systems, the anions from PCE adsorb on the surface of cement, resulting in electrostatic repulsion. At the same time, the side chains of PCE stretch out into the pore solution, resulting in steric hindrance. Due these two effects, the cement particles get very well dispersed and a water-reducing effect is achieved [65]. The dosage of HRWR was optimized by measuring the efflux time using Marsh cone. Similarly, the dosage of VMA was optimized by measuring the volume of bleed–water in the wick-induced bleed test. These two tests were carried out in parallel as both the dosages of HRWR and VMA can affect the fluidity and bleed resistance. A balance between the dosages of HRWR and VMA is necessary to achieve a grout with excellent fluidity and bleed resistance.

4.1.2. Fluidity & its retention and bleed resistance of PBG1 & 2

According to EN 447 [66], the efflux time and spread diameter (field-oriented test parameters to measure fluidity) immediately after mixing should not be more than 25 s and 140 mm, respectively. Fig. 7(a) shows the efflux time of all the PBGs immediately after mixing. PBG1 exhibited the lowest efflux time among all the PBGs – indicating the highest fluidity. The enhanced fluidity can be attributed to the ball bearing action provided by the spherical fly ash particles [25]. As per EN 447 [66], the percentage change in fluidity, at 30 min after the mixing, should not be more

Table 3
Mixture proportion, fresh and hardened properties of the PBGs.

	Material/Parameter	PBG1	PBG2	PBG3	PBG4	PBG5	PBG6
Mixture proportion (kg/m^3)	OPC	1088	1119	951	951	951	935
	FaF1	512	0	317	317	317	311
	FaF2	0	480	317	317	317	311
	Water	432	432	428	428	428	420
	HRWR	1.44	1.43	1.43	1.43	1.43	1.43
	VMA	0.80	0.79	0.50	0.80	0.63	0.63
	SRA	0	0	0	0	0	31.7
Fresh properties	$T_{e,\ 0}$ (s)	12	14	18	22	20	17
	$T_{e,\ 30}$ (s)	13	15	19	23	21	22
	$T_{e,\ 180}$ (s)	18.5	23.5	25	32.5	31	28
	$D_{s,\ 0}$ (mm)	167	158	151	146	155	159
	$D_{s,\ 30}$ (mm)	161	153	146	141	147	148
	$D_{s,\ 180}$ (mm)	130	127	113	121	123	134
	τ_0 (Pa)	–	–	–	15.79	8.11	6.46
	η_1(Pa.s^n)	–	–	–	0.30	0.34	0.21
	η_2(Pa.s^n)	–	–	–	0.24	0.29	0.11
	$BV_{Standard}$ (mm)	0.9	0.6	0.05	0	0	0
	$BV_{Wick\text{-}induced}$ (%)	1.5	1.2	0.1	0	0	0
	$BV_{Pressure,\ 350}$ (%)	0.4	0.5	0.1	0.1	0.1	0.1
	$BV_{Inclined}$ (%)	–	–	0.1	0.0	0.0	0.0
	$ST_{Initial}$ (hours)	4.8	5.1	5.3	6.5	6.4	7.8
	ST_{Final} (hours)	13.5	13.8	14.1	14.1	14.0	16.4
Hardened properties	ΔL (%)					−0.036	−0.016
	$AS_{70\text{-}day}$ ($\mu\varepsilon$)	–	–	–	–	503	163
	$TS_{70\text{-}day}$ ($\mu\varepsilon$)	–	–	–	–	816	339
	$f_{c,\ 3\text{-}day}$ (MPa)	28	31	32	28	30	26
	$f_{c,\ 7\text{-}day}$ (MPa)	42	43	45	46	47	41
	$f_{c,\ 28\text{-}day}$ (MPa)	69	67	69	66	68	62
	$V_{softgrout}$	0	0	0	0	0	0

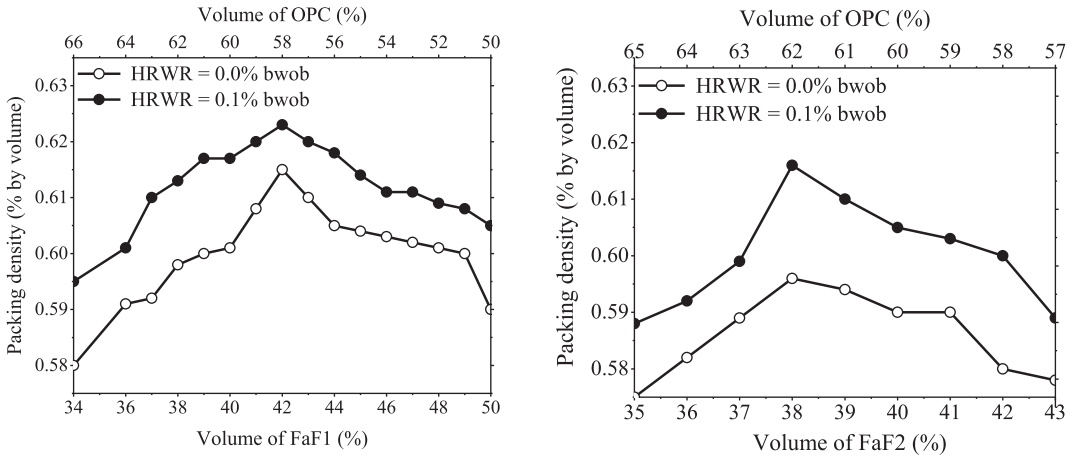

a) Blends of OPC and FaF1 b) Blends of OPC and FaF2

Fig. 6. Packing density of different blends of OPC, FaF1, and FaF2 combinations.

than 20%. Fig. 7(b) shows the percentage change in fluidity measured up to three hours after mixing; PBGs 1 & 2 have exhibited good retention of fluidity and satisfied the acceptance criterion. It was observed that the change in efflux time was more than the change in the spread for all the PBGs. This indicates that the Marsh cone test is more sensitive to the changes in fluidity than the spread test.

According to EN 447 [66], the acceptable limit for the wick-induced bleed is 0.3%. At the same time, PTI M5.1–12 specifies that the acceptable limit for pressure-induced bleed is 0.1% [50]. Fig. 8 shows the standard, wick-induced and pressure-induced bleed (at a maximum pressure of 350 kPa) test results. From Fig. 8, it is clear that the PBGs 1 & 2 exhibited high bleeding and thus do not satisfy the acceptance criteria for all the three different bleeding conditions.

4.2. Phase II – PBG 3

It was observed that the PBG1 and PBG2 grouts developed in Phase I do not have the needed bleed resistance, though they have exhibited good fluidity. Therefore, investigations were further continued to develop a bleed resistant and yet flowable grout without the tendency to form softgrout. For that purpose, different combinations and proportions of materials were examined. Phase II deals with the details of these further investigations.

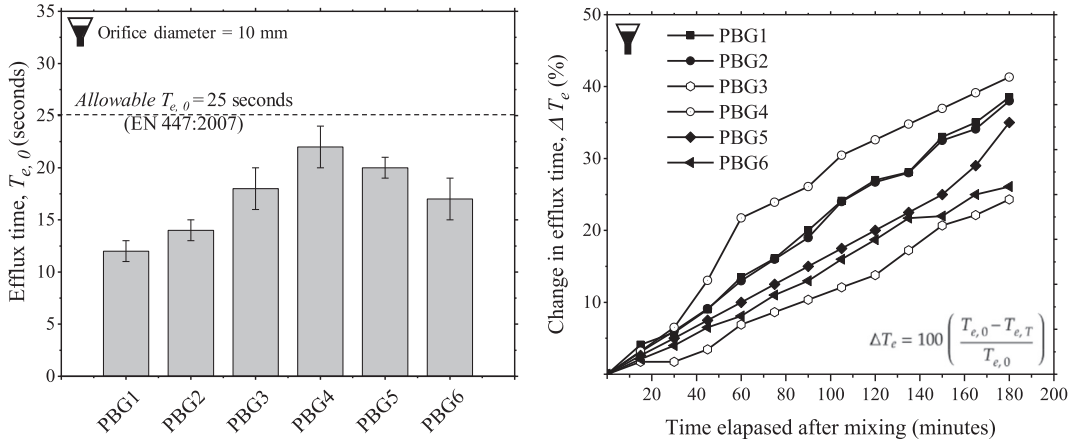

a) Efflux time ($T_{e,0}$) immediately after mixing

b) Retention of efflux time ($\Delta T_{e,0}$) up to three hours after mixing

Fig. 7. Efflux time and its retention of PBGs measured using the Marsh cone test.

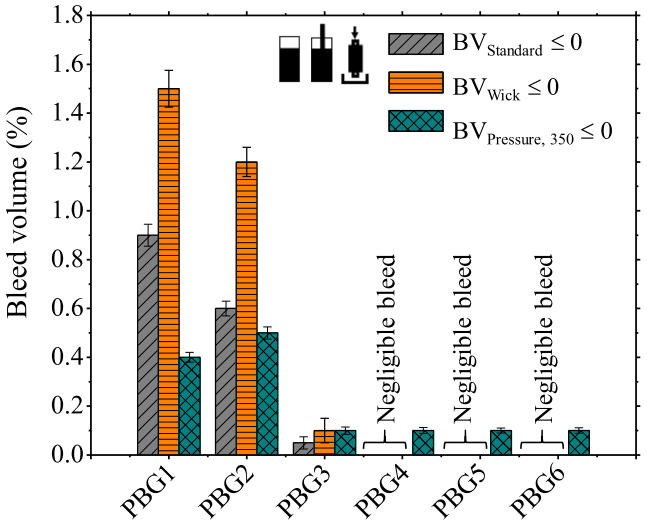

Fig. 8. Standard, wick-induced and pressure-induced bleed volume of PBGs.

4.2.1. Mixture proportioning of PBG3

Two different fly ashes with different particle sizes were used in the design of PBG3. As discussed earlier, the particles packing approach and Puntke tests was used for the design of PBG3. Table 4 lists the packing densities of the combinations of OPC, FaF1, and FaF2. From Table 4, it is clear that the packing density was maximum when the binders were in a volume proportion of 58:24:24. After optimising the volume proportion of the binders, the w/b was decided based on the water demand for the normal consistency. Then, the dosages of the HRWR and VMAs were optimised using the Marsh cone test and the wick-induced bleed test.

4.2.2. Fluidity & its retention and bleed resistance of PBG3

The grouting operations at construction sites can prolong until about 3 h, and the grout should be workable during that period. The fluidity and its retention for up to three hours after the mixing were monitored, and the results are shown in Fig. 7(a) & (b). It is evident that PBG3 satisfies the acceptance criteria for fluidity (i.e., 25 s efflux time) and the retention of fluidity (i.e., changes in fluidity should not be more than 20% at 30 min after mixing) as per EN 447 [66].

Fig. 8 shows that PBG3 can exhibit excellent fluidity and also meet the acceptance criterion for bleed resistance. The presence of two types of fly ash enabled enhanced packing density of the mixture and also the appropriate dosages of chemical admixtures improved the excellent bleed resistance, without compromising the fluidity. On the other hand, PBGs 1 & 2 exhibited the highest bleed, though they have excellent fluidity. PBG 3 exhibited a measurable volume of bleed water at 3 h after mixing; however, it was well below the maximum allowable limit of 0.3% as per EN 447 [66]. Therefore, based on the fluidity and bleed performance, PBG3 has been chosen as the reference mix for Phase III, which

Table 4
Packing density of the ternary blends.

Binder composition ID	Quantity (% bvob)			Packing density (vol%)
	OPC	FaF1	FaF2	
BC1	50	30	20	0.668 (±0.009)
BC2	55	30	15	0.660 (±0.008)
BC3	58	24	24	0.673 (±0.009)
BC4	65	25	30	0.659 (±0.007)
BC5	70	20	10	0.648 (±0.009)
BC6	50	20	30	0.663 (±0.008)
BC7	55	15	30	0.654 (±0.007)
BC8	60	10	30	0.651 (±0.009)
BC9	65	10	25	0.645 (±0.009)
BC10	70	10	20	0.634 (±0.008)

Note: BC is the abbreviation for binder composition.

includes additional characterization tests and industrial production.

4.3. Phase III – PBGs 4, 5, and 6

PBG3 from Phase II has been taken as the reference mix, and the mixture design was further fine-tuned for obtaining the target properties. PBGs 4, 5 & 6 were blended in sequence in an industrial blending facility, each time with slight modification of the proportion.

4.3.1. Mixture proportioning and industrial-scale productions

PBGs 4 & 5 were obtained by modifying the dosage of VMA (from PBG3) while maintaining the dosage of HRWR to improve the bleed resistance (see Table 3). Then, SRA was introduced in PBG6 - to reduce the shrinkage deformations to the allowable limit. The dosage of SRA was optimized by measuring the surface tension of the liquid phase of fresh grout. Fig. 9 shows the variation of the surface tension of the grout liquid phase with respect to different SRA dosages. The rate of reduction of surface tension was very steep initially and gradually becomes asymptotic as the SRA dosage increases. The dosage of SRA was fixed at 2% bwob as the addition of SRA more than 2% bwob did not change the surface tension of the liquid phase significantly. After determining the dosage of SRA from the tensiometer studies, the shrinkage of the PBGs containing the SRAs was studied.

4.3.2. Fluidity & its retention of PBG 4, 5, and 6

Fig. 7 shows the efflux time and its variation for PBGs 4, 5 & 6 mixes. The high efflux time and low spread exhibited by PBG 4 can be due to the high dosage of VMA. The VMA increased the viscosity of the liquid phase and thus resulted in decreased fluidity. Also, PBG6 exhibited excellent fluidity, which can be due to the presence of SRA, that decreased the surface tension of the liquid phase [40]. All the PBGs satisfied the acceptance criteria of 25 s efflux time, and 140 mm spread diameter as per EN 447 [66]. Note that PBG6 with SRA exhibited about 10% increase in the fluidity compared to PBG5 without SRA and a similar proportion of other ingredients. Therefore, the increase in fluidity of PBG6 can be attributed to the presence of SRA in PBG6.

PBG4 exhibited lower retention of fluidity (during the first 3 h) than PBG5 and 6. This can be due to the higher rate of increase of yield stress in PBG4 than the other PBGs. PBGs 4, 5, & 6 exhibited good fluidity retention, and PBG3 has the highest change in fluidity among all the PBGs. PBG 4, 5, and 6 satisfied the acceptance criterion set by EN 447 [66].

4.3.3. Bleed resistance of PBG 4, 5, and 6

From Fig. 8, it is clear that the PBG 4, 5, & 6 exhibited negligible bleed in all the three different simulated bleed conditions. This can be attributed to the presence of VMA, which increased the viscosity of the grout liquid phase – reducing the settling of cementitious phase. The All PBGs in Phase III passed the allowable bleed limit of 0.3%, as per EN 447 [66]. Fig. 8 shows the pressure-induced bleed test results. PBG 3, 4, 5 and 6 met the PTI requirement of less than 0.3% bleeding [50]).

The results of the inclined tube bleed test on PBG 3, 4, 5 and 6 are given in Table 3. Only PBG 3 exhibited a 0.1% bleed volume at 3 h after mixing, which is below the maximum allowable limit of 0.3% as per EN 447 [66]. PBG 4, 5, and 6 exhibited negligible bleeding, which can be due to the combined effect of VMA and SRA – although the SRA might have had lesser effect on this than VMA. As time passes, the SRA concentration in the liquid phase increases due to the consumption of water for the hydration [40]. As recommended by PTI and EN standards, the volume of bleed water was measured at three hours after mixing. By this time, the SRA concentration in liquid phase could have crossed the critical micelle concentration (CMC) and triggered the micelle formation. Beyond the CMC, the SRA molecules create micelles rapidly, which could have reduced the bleeding, segregation and settlement of cementitious particles.

4.3.4. Dimensional stability of PBG 5 and 6

The PT grouts in structures are in sealed condition because they are kept inside the plastic ducts. In such cases and for low w/b grouts with high paste volume, the autogenous shrinkage (AS) during the first 24 h are critical. Hence, this study focused on the autogenous shrinkage strains due to the addition of SRA. Note that the deformations during the initial 24 h (due to settlement, thermal contraction, plastic shrinkage, etc.) were not captured in the shrinkage strain measurements. The shrinkage strains were measured until the curve becomes asymptotic to the time axis. In general, this happened at about 70 days after casting of specimens. The evolution of total and autogenous shrinkage strains (square and triangular markers, respectively) in the prismatic grout specimens are shown in Fig. 10. With the addition of 2% bwob SRA, the autogenous shrinkage and total shrinkage at 70 days of age were reduced by 31% and 34%, respectively. Fig. 10 shows that the

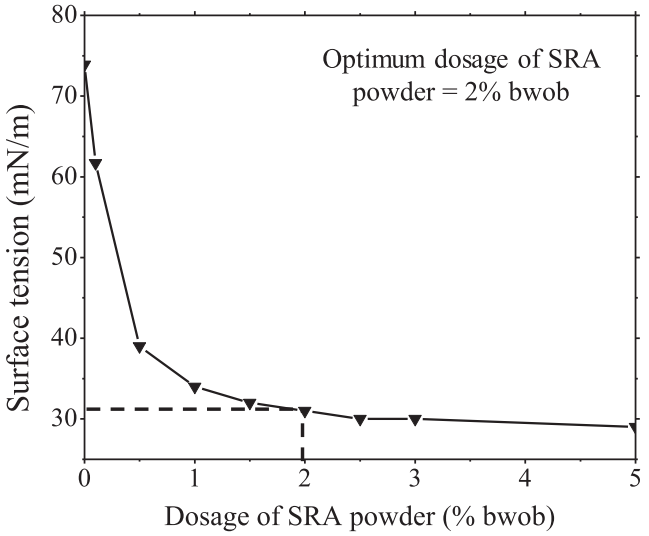

Fig. 9. Variation in surface tension of the grout liquid phase with SRA dosage.

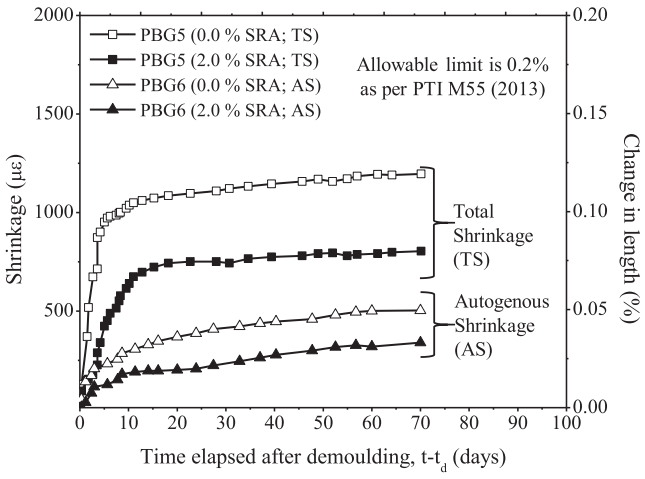

Fig. 10. Shrinkage deformations of PBG5 and PBG6 (t_d = 1 day).

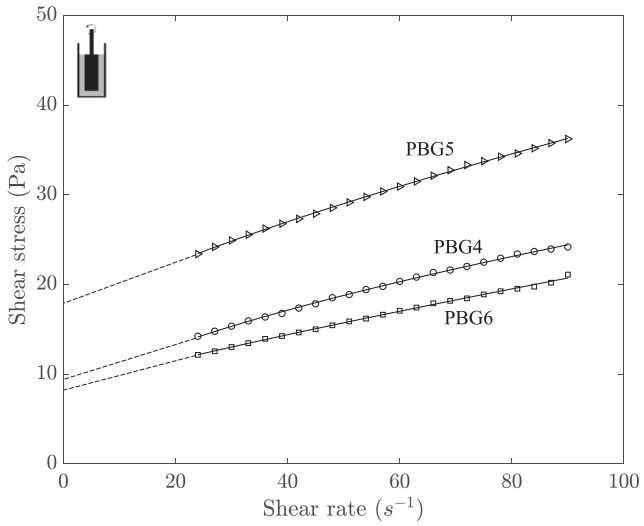

Fig. 11. Flow curve of PBGS.

autogenous shrinkage and the change in length (ΔL) of PBG6 (at 28 days) was about 160 μm and 0.016%, respectively, meeting the 0.2% criterion given in PTI M55.1–22 [50].

4.3.5. Set/hardened/softgrout properties of PBG 4, 5, and 6

Table 3 provides the setting times and cube compressive strengths of the PBGs. PBG6 exhibited the longest setting time due to the delay in hydration reaction by the reduced dissolution of alkali ions, adsorption of admixture on cement particles and the bond between the hydration products by the addition of SRA and other chemical admixtures [40]. The cube compressive strengths of all the PBGs were similar at 3, 7 and 28 days of curing. Recently, the minimization of softgrout formation is considered to be essential to achieve corrosion resistance and durability [30,30]. As suggested by Hamilton et al. [29], the top surface of the grout cylinder was scraped and visually observed. The volume of softgrout ($V_{softgrout}$), was found to be zero for PBG1 to 6.

4.3.6. Rheological behaviour of PBG 4, 5, and 6

Fig. 11 shows the flow curves of PBG 4, 5 and 6. A good fit is possible with Herschel-Bulkley model. Cementitious grout with high dosages of VMA, SRA, HRWR and low w/b is reported to exhibit the characteristics of the Herschel-Bulkley fluid [68,68]. The yield stress (τ_0) was determined by extrapolating the flow curves to the shear stress axis (ordinate) and measuring the shear stress corresponding to zero shear rate. Yield stress determined in this manner for PBG 4, 5 and 6 and the values are given in Table 3. It is clear that PBG5 has the highest yield stress and the highest bleed resistance, which is in agreement with the literature [69]. The apparent viscosity at low shear rate of 24 s^{-1} (η_1) and high shear rate of 90 s^{-1} (η_2) are given in Table 3. The apparent viscosity reduces as the shear rate increases – indicating shear thinning behaviour in all the PBGs tested. PBG6 exhibited very high bleed resistance, the lowest yield stress and apparent viscosity. Literature indicate that cementitious mixtures having lower yield stress and viscosity could result in lower pumping pressures [71–72]. Significantly low pumping pressures will result into the easier flow of grout through the ducts congested with multiple strands.

4.4. Performance specifications for PT grouts

Table 5 provides a set of comprehensive and stringent performance specifications for the qualification of grouts – combining the best of existing specifications by EN and PTI [19,50], and inputs from the current study. The three additional specifications from the current study are on the retention of fluidity and softgrout resistance. The specifications on the retention of fluidity (i.e., $T_{e,\ 180}$ and $D_{s,\ 180}$) are incorporated to ensure that the grout will have sufficient flow properties during the entire grouting process (say, about 3 h). These are important to ensure complete filling of the long ducts. Also, $V_{softgrout}$ = 0 is a recommendation from this study, which is important to ensure that grout does not segregate and softgrout is not accumulated at the high points such as anchorage zones. The PBG6 developed in this study meets all these stringent performance specifications, and is recommended for grouting of post-tensioned systems.

5. Summary and conclusions

This study focused on developing pre-blended cementitious grouts for post-tensioned concrete structures. The study was conducted in three phases. Phases I and II studied three grout mixes and their fluidity and bleed resistance properties. Then, these mixes were fine-tuned in the Phase III, where the mixture proportions were optimized and the various additional properties were

Table 5
Recommended specifications for the PT grouts (Note: PBG6 meets all these).

Parameter	Recommended performance specifications	Reference standard
$T_{e,\ 0}$ (s)	$T_{e,\ 0} \leq 25$	*EN 447 (2007) and from this study*
$T_{e\ 30}$ (s)	$1.2\ T_{e,\ 0} \geq T_{e\ 30} \geq 0.8\ T_{e,\ 0}$ & $T_{e\ 30} \leq 25$	
$T_{e,\ 180}$ (s)	**$1.4\ T_{e,\ 0} \geq T_{e,\ 180} \geq 0.8\ T_{e,\ 0}$ & $T_{e,\ 180} \leq 25$**	
$D_{s,\ 0}$ (mm)	$D_{s,\ 0} \geq 140$	
$D_{s,\ 30}$ (mm)	$1.2\ D_{s,\ 0} \geq D_{s,\ 30} \geq 0.8\ D_{s,\ 0}$ & $D_{s,\ 30} \geq 140$	
$D_{s,\ 180}$ (mm)	**$1.4\ D_{s,\ 0} \geq D_{s,\ 180} \geq 0.6\ D_{s,\ 0}$ & $D_{s,\ 180} \geq 140$**	
$BV_{Standard}$ (%)	≤ 0.10	*PTI M55. 1–12 (2013)*
BV_{Wick} (%)	≤ 0.30	*EN 447 (2007)*
$BV_{Pressure,\ 350}$ (%)	≤ 0.10	*PTI M55. 1–12 (2013)*
$BV_{Inclined}$ (%)	≤ 0.30	*EN 447 (2007)*
$ST_{Initial}$ (hr.)	≥ 3.0 and ≤ 12.0	*PTI M55. 1–12 (2013)*
ST_{Final} (hr.)	≤ 24.0	
$f_{c,\ 7\text{-day}}$ (MPa)	≥ 21	
$f_{c,\ 28\text{-day}}$ (MPa)	≥ 35	
ΔL (%)	$0 \leq \Delta L\ (\%) \leq 0.1$ at 1 day and $-0.2 \leq \Delta L\ (\%) \leq 0.2$ at 28 days	
$V_{softgrout}$	**= 0 (zero)**	*From this study*

Note: Recommendations on $T_{e,\ 180}$, $D_{s,\ 180}$, and $V_{softgrout}$ are from this study are in bold text.

investigated. The Phase III developed a grout (PBG6), which meets the best performance specifications of EN and PTI, and additional specifications on the retention of fluidity and resistance against softgrout formation, which are important to achieve zero-void and zero-softgrout conditions inside the ducts, which in turn will help achieve enhanced corrosion resistance of PT structures. Also, a set of stringent specifications by combining the best of EN and PTI specifications, and inputs from this study have been developed for qualifying PT grouts. The major conclusions from this study, for the materials and conditions considered here, are as follows.

- Maximizing the packing density can help in achieving the desired flow and bleed characteristics for cementitious grouts. The maximum possible packing density was seen to be about 68%, when 48% of OPC is replaced by a combination of two types of fly ashes.
- A grout with binders at maximum packing density and high range water reducer (HRWR) and viscosity modifying agent (VMA) at their optimal dosages could yield excellent fluidity and bleed resistance, without the formation of softgrout.
- The use of an SRA could reduce the autogenous and drying shrinkage significantly, and nominally increase the fluidity without affecting the bleeding resistance of the grouts.
- A grout with 48% OPC and 52% fly ash at a water-to-binder ratio of 0.27 and balanced dosages of HRWR, VMA and SRA could exhibit excellent flow properties and its retention for about 3 h, and good resistance against segregation (formation of bleedwater and softgrout), shrinkage, etc. without compromising the mechanical properties.

CRediT authorship contribution statement

Manu K. Mohan: Conceptualization, Data curation, Formal analysis, Investigation, Methodology, Supervision, Validation, Visualization, Writing - original draft, Writing - review & editing. **Radhakrishna G. Pillai:** Conceptualization, Funding acquisition, Methodology, Supervision, Project administration, Resources, Writing - review & editing. **Manu Santhanam:** Conceptualization, Funding acquisition, Methodology, Supervision, Project administration, Resources, Writing - review & editing. **Ravindra Gettu:** Conceptualization, Funding acquisition, Methodology, Supervision, Project administration, Resources, Writing - review & editing.

Declaration of Competing Interest

The authors declare that they have no known competing financial interests or personal relationships that could have appeared to influence the work reported in this paper.

Acknowledgements

This research was conducted as a part of the IMPRINT India initiative, Project No. 7711. Authors thank the Ministry of human resources development, Ministry of Urban Poverty Alleviation of Government of India for financial support. The authors also extend their gratitude towards Ultratech Cements Limited and L&T Construction for being the industrial partners of the project. The assistance from the technicians at the Construction Materials Research Laboratory and Sophisticated Analytical Instrument Facility at Indian Institute of Technology Madras is acknowledged. The assistance from Prof. J. Murali Krishnan and technicians in the Asphalt Laboratory for conducting the rheological experiments is also thankfully acknowledged.

References

[1] H.B. Wang, A.A. Sagues, R.G. Powers, Corrosion of the strand- anchorage system in post-tensioned grouted assemblies title, NACE Int. Corros. Conf. (2005) 1–20.
[2] Concrete society, Durable post-tensioned concrete bridges, Camberley, Surrey, UK, 1996.
[3] A.J. Schokker, B.D. Koester, J.E. Breen, M.E. Kreger, Development of High Performance Grouts for Bonded Post-Tensioned Structures, 1999.
[4] R. Helmerich, A. Zunkel, Partial collapse of the Berlin Congress Hall on May 21st, Eng. Fail. Anal. 43 (2014) (1980) 107–119, https://doi.org/10.1016/j.engfailanal.2013.11.013.
[5] R.J. Woodward, F.W. Williams, Collapse of Ynys-y-Gwas bridge, West Glamorgan (1988) 635–669.
[6] A. Arullappan, Mandovi river bridge collapse – A case Study, (2012). http://in.viadeo.com/en/groups/detaildiscussion/?containerId=002ltyqhsq8r9f7&forumId=0021en6cef18a5o1&action=messageDetail&messageId=0022bhq5gecjakpc (accessed May 18, 2020).
[7] B. Mathy, Investigation and strengthening study of twenty damaged bridges – A Belgium case history, in, Intl Conf Bridg. Manag. (1996).
[8] F.D.O.T. Report, Sunshine skyway bridge post-tensioned tendons investigation, Florida Department of Transportation, Tallahassee, FL, USA, 2001.
[9] F.D.O.T. Report, Corrosion evaluation of post-tensioned tendons on the Niles Channel bridge, Florida Department of Transportation, Tallahassee, FL, USA, 1999.
[10] C. Sly, An Initial Look at the Lowe's Motor Speedway Pedestrian Bridge Collapse, Pract. Fail. Anal. 1 (2001) 7–9.
[11] F.D.O.T. Report, Mid-Bay bridge post-tensioning evaluation-Final report, Florida Department of Transportation, Tallahassee, FL, USA, 2001.
[12] B. Hansen, Forensic engineering: Tendon failure raises questions about grout in post-tensioned bridges, Civ. Eng. 77 (2007) 17–18.
[13] S. Permeh, K. Vigneshwaran, K. Lau, Corrosion of post tensioned tendons with deficient grout, Florida Department of Transportation, Tallahassee, FL, USA, 2016.
[14] D. Trejo, R.G. Pillai, M.B.D. Hueste, K.F. Reinschmidt, P. Gardoni, Parameters influencing corrosion and tension capacity of post-tensioning strands, ACI Mater. J. 106 (2009) 144–153. 10.14359/56461.
[15] A. Sagues, R.G. Powers, H. Wang, Mechanism of corrosion of steel strands in post-tensioned grout assemblies, Corrosion. 1–15 (2003).
[16] P. Gardoni, R.G. Pillai, M.B.D. Hueste, K. Reinschmidt, D. Trejo, Probabilistic Capacity Models for Corroding Posttensioning Strands Calibrated Using Laboratory Results, J. Eng. Mech. 135 (9) (2009) 906–916, https://doi.org/10.1061/(ASCE)EM.1943-7889.0000021.
[17] R. Pillai, Electrochemical characterization and time-variant structural reliability assessment of post-tensioned, segmental concrete bridges, Texas A&M University (2009).
[18] BS EN445, Grout for prestressing tendons - Test methods, 2007.
[19] ASTM:C939, Standard Test Method for Flow of Grout for Preplaced-Aggregate Concrete (Flow Cone Method), ASTM International, West Conshohocken, PA, USA, 2010. 10.1520/C0939-10.2.
[20] RD Hooton, KH Khayat, A. Yahia, Simple field tests to characterize fluidity and washout resistance of structural cement grout, Cem. Concr. Aggregates. 20 (1) (1998) 145, https://doi.org/10.1520/CCA10448J.
[21] A. Miltiadou-Fezans, T.P. Tassios, Fluidity of hydraulic grouts for masonry strengthening, Mater. Struct. Constr. 45 (12) (2012) 1817–1828, https://doi.org/10.1617/s11527-012-9872-8.
[22] R. Le Roy, N. Roussel, The marsh cone as a viscometer: Theoretical analysis and practical limits, Mater. Struct. 38 (2005) 25–30, https://doi.org/10.1007/bf02480571.
[23] C. Jayasree, J. Murali Krishnan, R. Gettu, Influence of superplasticizer on the non-Newtonian characteristics of cement paste, Mater. Struct. Constr. 44 (5) (2011) 929–942, https://doi.org/10.1617/s11527-010-9677-6.
[24] T.S. Krishnamoorthy, S. Gopalakrishnan, K. Balasubramanian, B.H. Bharatkumar, R.M.P. Rao, Investigations on the cementitious grouts containing SCM, Cem. Concr. Res. (2002).
[25] K.H. Khayat, A. Yahia, M. Sayed, Effect of supplementary cementitious materials on rheological properties, bleeding, and strength of structural grout, ACI Mater. J. 105 (2008) 585–593. 10.14359/20200.
[26] T. Cheewaket, C. Jaturapitakkul, W. Chalee, Long term performance of chloride binding capacity in fly ash concrete in a marine environment, Constr. Build. Mater. 24 (8) (2010) 1352–1357, https://doi.org/10.1016/j.conbuildmat.2009.12.039.
[27] R.K. Dhir, M.R. Jones, Development of chloride-resisting concrete using fly ash, Fuel. 78 (2) (1999) 137–142, https://doi.org/10.1016/S0016-2361(98)00149-5.
[28] S. Kamalakannan, R. Thirunavukkarasu, R.G. Pillai, M. Santhanam, Factors affecting the performance characteristics of cementitious grouts for post-tensioning applications, Constr. Build. Mater. 180 (2018) 681–691, https://doi.org/10.1016/j.conbuildmat.2018.05.236.
[29] H.R. Hamilton, A. Piper, A. Randell, B. Brunner, Simulation of Prepackaged Grout Bleed under Field Conditions, (2014).
[30] A. Randell, M. Aguirre, H.R. Hamilton, Effects of low reactivity fillers on the perfomance of post-tensioning grout, PTI J. (2015).
[31] M. Schupack, Admixture for Controlling Bleed in Cement Grout Used in Post-Tensioning, PCI J 19 (6) (1974) 28–39.

[32] ASTM:C1741, Standard Test Method for Bleed Stability of Cementitious Post-Tensioning Tendon, 2011. 10.1520/C1741-11.
[33] A.J. Schokker, H.R. Hamilton, M. Schupack, Estimating post-tensioning grout bleed resistance using a pressure-filter test, PCI J. 47 (2) (2002) 32–39.
[34] K.H. Khayat, Viscosity enhancing admixtures for cement based materials-An overview, Cem. Concr. Compos. 22 (1998) 18–24, https://doi.org/10.1061/(ASCE)MT.1943-5533.0000026.
[35] K.H. Khayat, A. Yahia, Effect of welan gum-high-range water reducer combinations on rheology of cement grout, ACI Mater. J. 94 (1997) 365–372.
[36] A.V. Rahul, M. Santhanam, H. Meena, Z. Ghani, 3D printable concrete: Mixture design and test methods, Cem. Concr. Compos. 97 (2019) 13–23, https://doi.org/10.1016/j.cemconcomp.2018.12.014.
[37] A.V. Rahul, A. Sharma, M. Santhanam, A desorptivity-based approach for the assessment of phase separation during extrusion of cementitious materials, Cem. Concr. Compos. 108 (2020), https://doi.org/10.1016/j.cemconcomp.2020.103546 103546.
[38] M. Carsana, L. Bertolini, Characterization of Segregated Grout Promoting Corrosion of Posttensioning Tendons, J. Mater. Civ. Eng. 28 (2016) 1–9, https://doi.org/10.1061/(ASCE)MT.1943-5533.0001451.
[39] T. Terzioglu, M.M. Karthik, S. Hurlebaus, M.B.D. Hueste, S. Maack, J. Woestmann, H. Wiggenhauser, M. Krause, P.K. Miller, L.D. Olson, Nondestructive evaluation of grout defects in internal tendons of post-tensioned girders, NDT E Int. 99 (2018) 23–35, https://doi.org/10.1016/j.ndteint.2018.05.013.
[40] F. Rajabipour, G. Sant, J. Weiss, Interactions between shrinkage reducing admixtures (SRA) and cement paste's pore solution, Cem. Concr. Res. 38 (5) (2008) 606–615, https://doi.org/10.1016/j.cemconres.2007.12.005.
[41] E. Tazawa, S. Miyazawa, Influence of cement and admixture on autogenous shrinkage of cement paste, Cem. Concr. Res. 25 (2) (1995) 281–287, https://doi.org/10.1016/0008-8846(95)00010-0.
[42] J. Mora-Ruacho, R. Gettu, A. Aguado, Influence of shrinkage-reducing admixtures on the reduction of plastic shrinkage cracking in concrete, Cem. Concr. Res. 39 (3) (2009) 141–146, https://doi.org/10.1016/j.cemconres.2008.11.011.
[43] R. Gettu, J. Roncero, Behaviour of concretes with shrinkage reducing admixtures, in: Y. Yuan, S.P. Shah, H.-L.- Lü (Eds.), ICACS 2003, RILEM Publications, Bagneux, France, 2003: pp. 11–20.
[44] K.J. Folliard, N.S. Berke, Properties of high-performance concrete containing shrinkage-reducing admixture, Cem. Concr. Res. 27 (9) (1997) 1357–1364, https://doi.org/10.1016/S0008-8846(97)00135-X.
[45] G. Sant, B. Lothenbach, . Juilland, G. Le Saout, J. Weiss, K. Scrivener, The origin of early age expansions induced in cementitious materials containing shrinkage reducing admixtures, Cem. Concr. Res. 41 (3) (2011) 218–229, https://doi.org/10.1016/j.cemconres.2010.12.004.
[46] D.P. Bentz, Influence of Shrinkage-Reducing Admixtures on Early-Age Properties of Cement Pastes, J. Adv. Concr. Technol. 4 (3) (2006) 423–429, https://doi.org/10.3151/jact.4.423.
[47] R. Gettu, J. Roncero, M.A. Martin, Long-term behaviour of concrete incorporating a shrinkage-reducing admixture, Indian Concr. J. 76 (2002) 586–592.
[48] D.Y. Yoo, G.S. Ryu, T. Yuan, K.T. Koh, Mitigating shrinkage cracking in posttensioning grout using shrinkage-reducing admixture, Cem. Concr. Compos. 81 (2017) 97–108, https://doi.org/10.1016/j.cemconcomp.2017.05.005.
[49] BIS (Bureau of Indian Standards), Specification for 53 grade ordinary portland cement, 2013.
[50] PTI M55.1-12, Specification for Grouting of Post-Tensioned Structures, 2002.
[51] ASTM:C1738, Standard Practice for High-Shear Mixing of Hydraulic Cement Pastes, ASTM International, West Conshohocken, PA, USA, 2019. 10.1520/C1738_C1738M-19.
[52] ASTM:D1331, Standard Test Methods for Surface and Interfacial Tension of Solutions of Surface-Active Agents, and Related Materials, West Conshohocken, PA, USA, 2014. 10.1520/D1331-14.
[53] ASTM C157, StandardTest Method for Length Change of Hardened Hydraulic-Cement Mortar and Concrete, ASTM International, West Conshohocken, PA, USA, 2016. 10.1520/C0157_C0157M-17.
[54] ASTM:C953, Standard Test Method for Time of Setting of Grouts for Preplaced-Aggregate Concrete in the Laboratory, ASTM International, West Conshohocken, PA, USA, 2010. 10.1520/C0953-10.2.
[55] ASTM:C942, Standard Test Method for Compressive Strength of Grouts for Preplaced-Aggregate Concrete in the Laboratory, ASTM International, West Conshohocken, PA, USA, 2010. 10.1520/C0942-99R04.2.
[56] L. Ferrara, M. Cremonesi, N. Tregger, A. Frangi, S.P. Shah, On the identification of rheological properties of cement suspensions: Rheometry, Computational Fluid Dynamics modeling and field test measurements, Cem. Concr. Res. 42 (2012) 1134–1146, https://doi.org/10.1016/j.cemconres.2012.05.007.
[57] F. de Larrard, C.F. Ferraris, T. Sedran, Fresh concrete : A Herschel-Bulkley material, Mater. Struct. 31 (1998) 494–498, https://doi.org/10.1007/BF02480474.
[58] V.-H. Nguyen, Sébastien Remond, J.-L. Gallias, Influence of cement grouts composition on the rheological behaviour, Cem. Concr. Res. 41 (3) (2011) 292–300, https://doi.org/10.1016/j.cemconres.2010.11.015.
[59] D.P. Bentz, C.F. Ferraris, M.A. Galler, A.S. Hansen, J.M. Guynn, Influence of particle size distributions on yield stress and viscosity of cement-fly ash pastes, Cem. Concr. Res. 42 (2) (2012) 404–409, https://doi.org/10.1016/j.cemconres.2011.11.006.
[60] P. Nanthagopalan, M. Haist, M. Santhanam, H.S. Müller, Investigation on the influence of granular packing on the flow properties of cementitious suspensions, Cem. Concr. Compos. 30 (9) (2008) 763–768, https://doi.org/10.1016/j.cemconcomp.2008.06.005.
[61] Elkem, User Guide Elkem Materials Mixture Analyser – EMMA, 2016.
[62] S.V. Kumar, M. Santhanam, Particle packing theories and their application in concrete mixture proportioning: A review, Indian Concr. J. 77 (2003) 1324–1331.
[63] C. Zhang, J. Yang, J. Fu, X. Ou, Y. Xie, X. Liang, Performance Evaluation of Modified Cement-Sodium Silicate Grouting Material for Prereinforcing Loose Deposit Tunnels, J. Mater. Civ. Eng. 31 (2019) 06019003, https://doi.org/10.1061/(asce)mt.1943-5533.0002747.
[64] C. Zhang, J. Fu, J. Yang, X. Ou, X. Ye, Y. Zhang, Formulation and performance of grouting materials for underwater shield tunnel construction in karst ground, Constr. Build. Mater. 187 (2018) 327–338, https://doi.org/10.1016/j.conbuildmat.2018.07.054.
[65] S. Sha, M. Wang, C. Shi, Y. Xiao, Influence of the structures of polycarboxylate superplasticizer on its performance in cement-based materials-A review, Constr. Build. Mater. 233 (2020), https://doi.org/10.1016/j.conbuildmat.2019.117257 117257.
[66] B.S. En, 447, Grout for prestressing tendons -, Basic requirements (2007).
[67] J. Liu, Y. Li, G. Zhang, Y. Liu, Effects of cementitious grout components on rheological properties, Constr. Build. Mater. 227 (2019), https://doi.org/10.1016/j.conbuildmat.2019.08.035 116654.
[68] G. Zhang, J. Liu, Y. Li, J. Liang, A pasty clay-cement grouting material for soft and loose ground under groundwater conditions, Adv. Cem. Res. 29 (2) (2017) 54–62, https://doi.org/10.1680/jadcr.16.00079.
[69] A. Perrot, T. Lecompte, H. Khelifi, C. Brumaud, J. Hot, N. Roussel, Yield stress and bleeding of fresh cement pastes, Cem. Concr. Res. 42 (7) (2012) 937–944, https://doi.org/10.1016/j.cemconres.2012.03.015.
[70] M.K. Mohan, A.V. Rahul, K. Van Tittelboom, G. De Schutter, Rheological and pumping behaviour of 3D printable cementitious materials with varying aggregate content, Cem. Concr. Res. 139 (2021) 3, https://doi.org/10.1016/j.cemconres.2020.106258.
[71] M.K. Mohan, A. V. Rahul, K. Van Tittelboom, G. De Schutter, Extrusion-based concrete 3D printing from a material perspective: a state-of-the-art review, Cem. Concr. Compos. (Accepted-in Press. (n.d.).
[72] M. Mohan, A. V Rahul, G. De Schutter, K. Van Tittelboom, Early age hydration, rheology and pumping characteristics of CSA cement-based 3D printable concrete, Constr. Build. Mater. (n.d.) 3.